Journal of Solid Mechanics and Materials Engineering

Vol. 4, No. 7, 2010

Electrical Resistance Change of CFRP under a Compression Load*

Akira TODOROKI**, Kensuke SUZUKI***, Yoshihiro MIZUTANI**
and Ryosuke MATSUZAKI**
** Department of Mechanical Sciences and Engineering, Tokyo Institute of Technology
2-12-1 Ookayama, Meguro-ku, Tokyo, Japan
E-mail:atodorok@ginza.mes.titech.ac.jp
*** Tokyo Institute of Technology

Abstract

Many researchers adopt electrical resistance change (ERC) methods to detect damage in Carbon Fiber Reinforced Plastic (CFRP) laminates. They usually apply the method under tensile or bending loads. For compression tests, a block type specimen is used. The block type specimen, however, is too thick to obtain a uniform electrical current. This study starts with the design of a compression test specimen with uniform electrical current using a sandwich beam specimen. The four-point bending tests revealed that the piezoresistivity of the compression tests was the same as that of the tension tests. Using a three-point bending test, fiber-micro-buckling was obtained, which caused an increase in electrical resistance with residual compression strain. Non-linear behaviors observed during cyclic loading tests were investigated, and it was revealed that the plastic deformation at the loading point had large effect.

Key words: Composites, Carbon, Compression, Electrical Resistance, Buckling

1. Introduction

Carbon Fiber Reinforced Plastics (CFRP) composites have been widely adopted not only for aerospace components but also in automobile structures because of the superior specific strength and specific stiffness. The CFRP structures, however, require automatic damage detection systems because it is quite difficult to find the damage visually for black structures made from the CFRP. Since carbon fibers are electrically conductive, self-sensing systems that utilize electrical resistance changes of the reinforcement fibers are the subject of attention from many researchers [(1)-(10)]. The method requires measurement of electrical resistance to detect damage or applied strain. Since the method uses the fibers as sensors, additional sensors are not required, thus the method is called self-sensing.

The authors' research group has undertaken research on electrical resistance change methods for monitoring applied strain, matrix cracking and delamination cracks [(11)-(17)]. However, little research has been done on compression tests using electrical resistance changes because of the difficulty of doing these tests. Mei et al., have done compression tests using electrical resistance change measurements on a block type specimen [(18)]. They revealed that the electrical resistance change caused by applied compression strain is different from that caused by tensile strain. They, however, used different specimen configurations for the compression tests to prevent buckling. Since the CFRP laminates have strongly orthotropic electrical conductivity, this might bring different results in

*Received 29 Mar., 2010 (No. 10-0129)
[DOI: 10.1299/jmmp.4.864]

electrical resistance changes for the tensile test. Wang and Chung have reported on the piezoresistivity of the compression test in their beam bending tests [19]. Since the bending test includes both compression and tensile strains in the beam, the results may include the effect of the tensile strain. Although a failure mode of compression tests is fiber micro-buckling, the electrical resistance change caused by the micro-buckling is not examined in detail.

This study deals with the electrical resistance change method (ERCM) of CFRP under compression loading. A sandwich bending specimen is designed using FEM analyses. A couple of thin unidirectional CFRP beams are attached to both surfaces of a GFRP beam. The electrical current density of the CFRP beam is analyzed using FEM, and the effect of the GFRP constraint on the piezoresistivity is investigated using the multi-axial loading piezoresistivity formula obtained in the previous paper [12]. Using the carefully designed sandwich beam specimens, four-point bending tests are performed to obtain the piezoresistivity of CFRP under compression and tension loading. Three-point bending tests are performed to examine the electrical resistance change caused by the fiber-micro-buckling.

2. Design of compression test specimen and tensing method

As previously mentioned, when a block type specimen is used for the unidirectional compression test to prevent global buckling, the electrical current density in the cross section of the block type specimen may not be uniform because of the highly orthotropic conductivity of CFRP. A bending type specimen has a compression side and a tension side. To separate the compression side from the tension side, the electrical insulator GFRP can be embedded in the middle of the bending specimen. Even for this specimen, strain distribution exists in the compression side. A sandwich type specimen enables us to obtain an isolated compression side with a small difference between the maximum compression strain and the minimum compression strain.

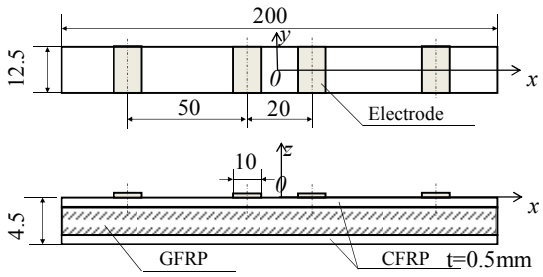

Fig. 1 Sandwich beam type specimen configuration

Figure 1 shows the configuration of the sandwich beam type specimen. The top and bottom surface CFRP beams are made from unidirectional CFRP: Toray T300/3601 prepreg # P3060-15. The cure condition of the prepreg is 180°C × 0.7 MPa × 6 hr. The stacking sequence is a four-ply unidirectional specimen. The CFRP beam is 0.5 mm thick. The core GFRP is a commercially available fabric GFRP 3 mm thick. For the bonding surface of the CFRP beams to the GFRP core, epoxy type adhesive, SW21 produced by Sumitomo 3M, is used. The total thickness of the beam is approximately 4.5 mm including the thickness of the adhesive layer. The fiber volume fraction of the CFRP beams is measured using JIS K7075: $V_f = 64$ %.

A four-probe method is adopted to prevent the electrical resistance change caused by debonding of the electrode. The electrode is made using an electrical copper plating method. The copper plating method is described in a previous paper [20]. The outer couple of electrodes are used for applying electrical current and the inner couple of electrodes are used for measurement of electrical voltage. To confirm the uniform electrical current, FEM

is applied. The results are described in the section 3.1.

Figure 2 shows the loading conditions for this research. The four-point bending test is adopted to measure the piezoresistivity of CFRP under compression loading. Using the same specimen, we can measure the piezoresistivity under tension loading by placing the specimen upside down. For the compression test, the tensile strain is measured by the strain gage, and the compression strain is measured by the strain gage for the tensile test. For the investigation of damage monitoring caused by compression loading, a three-point bending test is performed. Since the three-point bending test includes shear strain at the indentation point, this study measures the electrical resistance changes after unloading. The three-point bending test enables us to measure the electrical resistance change caused by fiber micro-buckling. To prevent electrical shorts, a Teflon film of 0.5 mm is inserted between the jig and the specimen. The strain gage is attached to the tensile side surface of the CFRP beam. The electrical resistance is measured using an LCR meter (Hytester 3522-50) produced by Hioki E.E. Co. Ltd. To measure the electrical resistance, a 30 mA alternating current of 450 Hz is used. Since the phase of the measured alternating current at 450 Hz is 0, the impedance does not include capacitance at this frequency.

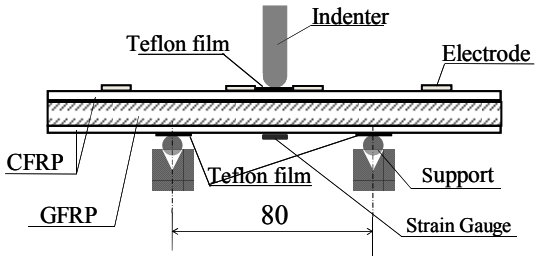

(b) Three-point bending test

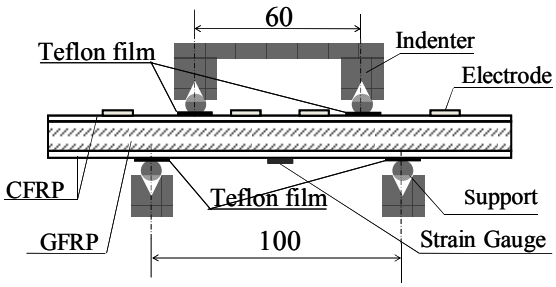

(a) Four-point bending test

Fig. 2 Bending test equipment set up

3. Results and discussion

3.1 FEM analysis of electrical current

The reference [15] provides the electrical conductivity ratio of CFRP for $V_f = 62$ %: $\sigma_t/\sigma_0 = 3.8\times10^{-3}$. The commercially available FEM code ANSYS is used for the FEM analysis. The coordinate of x-y-z is defined as shown in Fig. 3. The x-y coordinates are defined as the surface on the top of the CFRP beam. Figure 3 shows the FEM results of the electrical current density in the x-direction: 1 A is applied at x = -60mm, and the voltage is set to 0 at x = 60 mm. The abscissa shows the electrical current density in the x-direction and the ordinate is the distance from the surface of the top CFRP beam. The solid triangle symbols indicate the electrical current density of x = -50 mm (near the electrode for applying the electrical current). The open circle symbols indicate the electrical current density at x = -10 mm (under the electrode for measuring the electrical voltage). In this FEM analysis, the copper electrodes are not modeled into the FEM analysis.

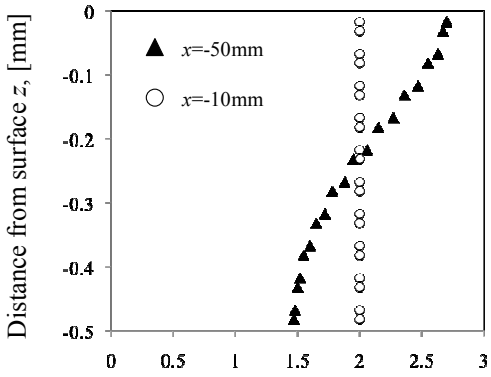

Fig. 3 Electrical current density in the x-direction

Figure 3 shows that the electrical current is uniform in the measured segment between the inner couple of electrodes although it is not uniform near the outer couple of the electrodes even for the thin CFRP beam. This means the electrical current can be assumed to be uniform for measurements of voltage change.

The GFRP used for the sandwich core includes glass fibers in the y-direction. To investigate the effect of the strain constraint caused by the GFRP on the piezoresistivity of the surface CFRP beam, 3-D strain analysis was performed. The total number of elements is 2,400, and the total number of nodes is 27,951. The material properties used for the FEM analysis are shown in Table 1.

Table 1 Material properties used for FEM analysis

GFRP	
E	11.9 GPa
G	5 GPa
ν	0.16
CFRP	
E_L	136 GPa
E_T	9 GPa
G_{LT}	7 GPa
ν_{LT}	0.35

Using the 3-D FEM analysis, the transverse strain ratios between $\varepsilon_{y,\,z=0}$ (the surface of the CFRP beam) and $\varepsilon_{y,\,z=-0.5}$ (the bottom of the CFRP beam) are obtained. The woven fabric GFRP has a smaller Poisson's ratio as shown in Table 1 because of the glass fibers in the transverse direction. The smaller Poisson's ratio brings a constraint on the shrinkage in the transverse direction of the surface CFRP beam. This effect can be analyzed by comparing the two FEM results: the first is a sandwich beam and the second is a pure CFRP beam of the same height. Figure 3 shows the results of the transverse strain ratios of the two cases. The solid curve is the result obtained from the pure CFRP beam of 4.5 mm height, and the dashed curve is the result obtained from the sandwich beam. The abscissa is the y-coordinate and the ordinate is the strain ratio between $\varepsilon_{y,\,z=0}$ and $\varepsilon_{y,\,z=-0.5}$.

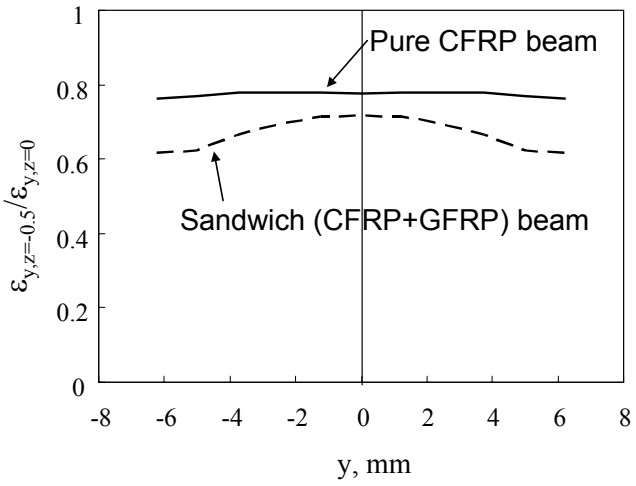

Fig. 4 Strain ratio of two FEM results in transverse direction

As shown in Fig. 4, the constraint causes the decrease of the transverse strain in the sandwich beam (dashed curve). The effect is, however, very small in the middle of the beam. Even at the edge of the beam (y = 6 mm or y = -6 mm), the decrease of the transverse strain due to the transverse constraint is less than 20 %. If we consider the transverse strain decreases by 20 % due to the constraint, we can estimate the maximum effect of the transverse constraint on the piezoresistivity. The multiaxial piezoresistivity has been published in reference [12]. The electrical resistance change ratio caused by the multiaxial strain is calculated as follows:

$$\begin{Bmatrix} \left(\frac{\Delta R}{R}\right)_L \\ \left(\frac{\Delta R}{R}\right)_T \end{Bmatrix} = \begin{bmatrix} 2.49 & 0.43 \\ -0.42 & 2.38 \end{bmatrix} \begin{Bmatrix} \varepsilon_L \\ \varepsilon_T \end{Bmatrix} \tag{1}$$

Let us consider the case of $\varepsilon_L = 0.01$ and $\varepsilon_T = -\nu_{LT}\varepsilon_L = -0.0035$. In this case, $(\Delta R/R)_L = 0.0234$. When the transverse strain shrinks by 20 %, $(\Delta R/R)_L = 0.0237$. The difference is only 1.3 %. This means the constraint in the transverse direction due to the glass fiber can be negligible for this type of specimen.

Since the longitudinal strain at the bottom surface (z = -0.5 mm) is 30 % smaller than the longitudinal strain at the surface (z = 0 mm), the averaged longitudinal strain is 15 % smaller than the surface strain. Using this type of specimen, we can measure the true piezoresistivity of compression strain and the electrical resistance change ratio caused by the compression loading.

3.2 Measured results and discussion

Figure 5 shows the results of cyclic loading using the four-point bending test. The abscissa is the measured strain using the strain gage attached to the tensile side. The ordinate is the measured electrical resistance change ratio. The solid curves show the results during loading and the broken curves show the results during unloading. Since the maximum load of this test is very small, the entire region is included in the elastic deformation region. Both tension and compression loading results show the linear behavior and the same slopes. This means the piezoresistivity under the compression loading is identical to that of tension loading at least up to the strain level of 500 $\times 10^{-6}$.

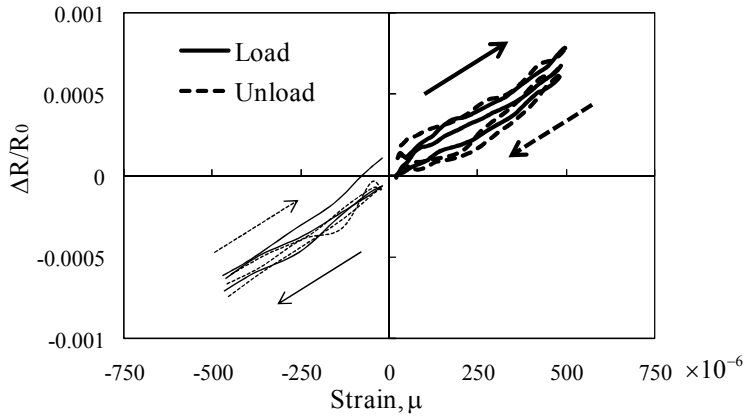

Fig. 5 Electrical resistance change up to 500×10^{-6} (R_0=93 mΩ)

When the applied strain exceeds 500×10^{-6}, the electrical resistance change ratio becomes non-linear as shown in Fig. 6. When loading, the electrical resistance change ratio decreases severely compared with the linear slope observed up to 500×10^{-6}. When unloading, however, the electrical resistance change ratio linearly decreases as shown by the broken line in Fig. 6. When reloading, the electrical resistance increases on the line observed during the unloading of the previous cycle. This mechanism is discussed later with additional experimental results.

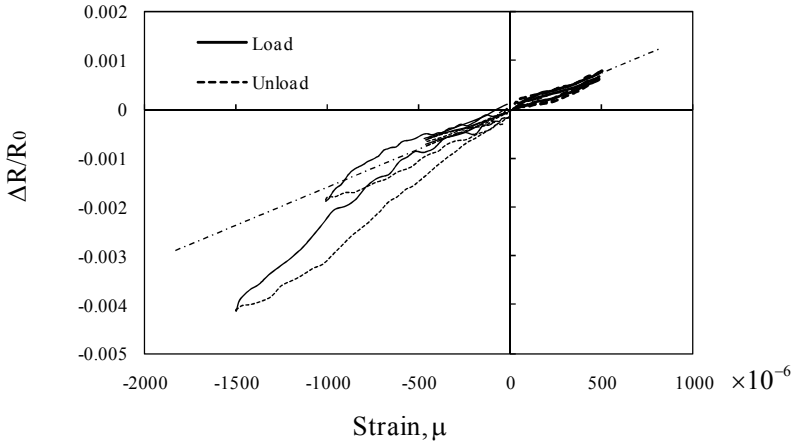

Fig. 6 Non-linear behavior observed over 500×10^{-6} (R_0=93 mΩ)

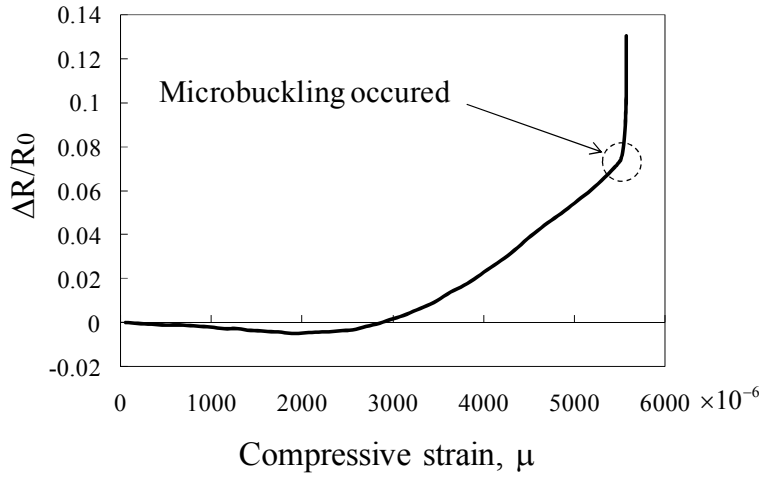

Fig. 7 Electrical resistance change up to the point of fiber micro-buckling (R_0 = 80 mΩ)

Three-point bending tests were performed to measure the electrical resistance change ratio caused by damage due to compression loading. The electrical resistance change ratio was measured up to the point of fiber-micro-buckling. The measured result is shown in Fig. 7. The abscissa is the applied strain, and the ordinate is the measured electrical resistance change ratio. As shown in Fig. 7, the electrical resistance change ratio decreases with the increase in the applied strain up to 2000 $\times 10^{-6}$. The electrical resistance change ratio increases over the applied strain of 2000 $\times 10^{-6}$. At the applied strain of 5500$\times 10^{-6}$, fiber-micro-buckling was observed. The micro-buckling results in a significant increase in electrical resistance change ratio. The cross sectional view of the fiber-micro-buckling is shown in Fig. 8.

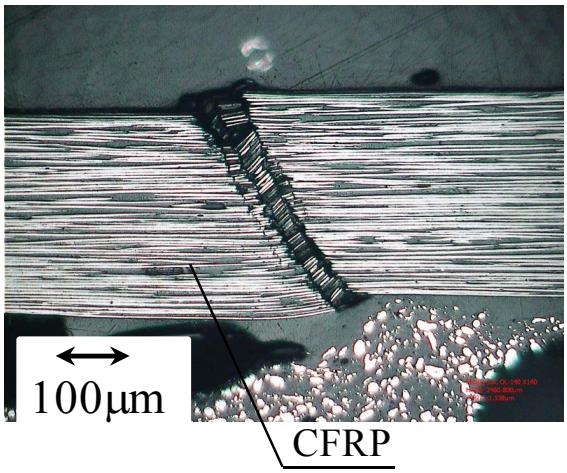

Fig. 8 Cross sectional view of fiber micro-buckling

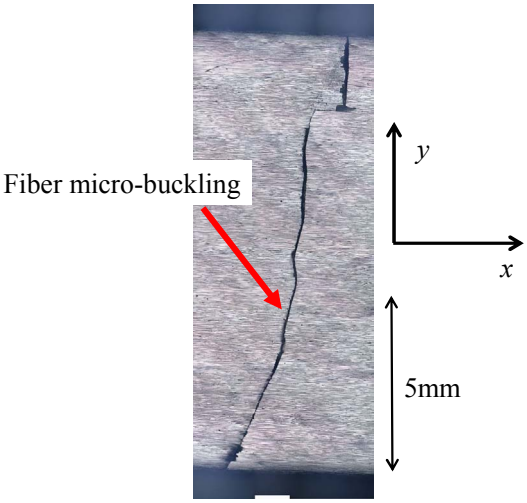

Fig. 9 Fiber micro-buckling from the specimen top

Figure 9 shows the fiber micro-buckling observed from the top of the specimen. As shown in Fig. 9, the micro-buckling occurs across the entire cross section of the top CFRP surface. The fiber micro buckling causes shrinkage of the CFRP. The specimen had approximately 2000 $\times 10^{-6}$ of residual compression strain in the completely unloaded condition. The micro-buckling causes an increase in electrical resistance from 80 mΩ to 128 mΩ. This means the micro-buckling causes an increase in electrical resistance of 48 mΩ. We now consider the initial length of the measured area at 20 mm, and the length of the area where micro-buckling occurs at 100 μm. Since the initial electrical resistance of the

100 μm wide area is approximately 0.4 mΩ, the resistivity ρ increases approximately 120 times as a result of the micro-buckling. Although the fiber micro-buckling breaks the carbon fibers, compression loading keeps the fiber contact between the broken fibers even after the completely unloading.

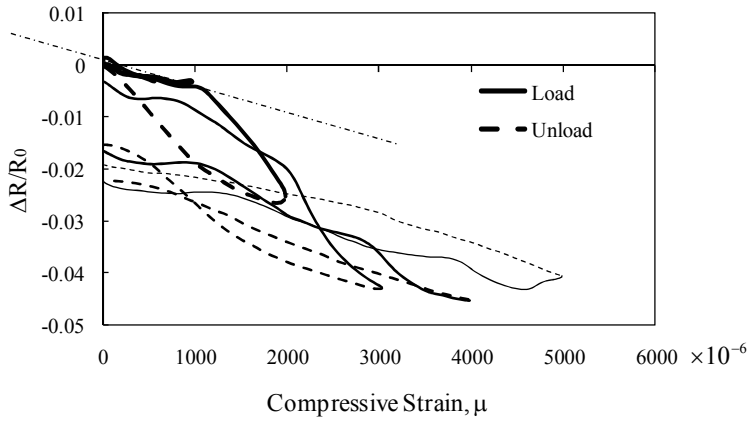

Fig. 10 Electrical resistance change ratio during loading-unloading of the three-point bending test over applied strain of 500×10^{-6}(R_0 = 112.5 mΩ)

Figure 10 shows the typical electrical resistance change ratio under cyclic loading of the three-point bending test over applied strain of 500×10^{-6}. In the four-point bending test, a non-linear relationship was observed over 500×10^{-6} as shown in Fig. 6. In the three-point bending test, the non-linear relationship is observed over 1000×10^{-6} as shown in Fig. 10. We assume the load at indentation is P. For the three-point bending test of this study, the applied moment at the strain gage position is $M_3 = (P/2) \times 40$ mm $= 20P$. For the four-point bending test of this study, the applied moment at the strain gage position $M_4 = P \times 20$ mm $= 20P$ (the total loading is $2P$). This means that the starting point of the non-linear behavior has the same indention load. This indentation load may affect the non-linear behavior. To confirm this indentation load effect, an indentation test was performed as shown in Fig. 11.

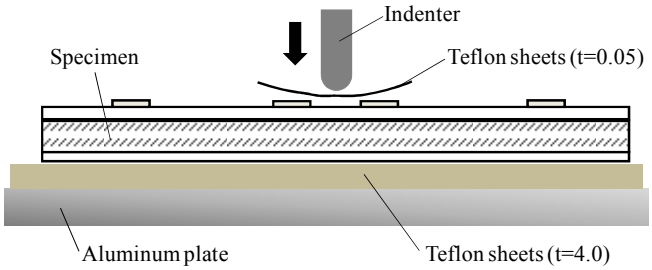

Fig. 11 Indentation test method

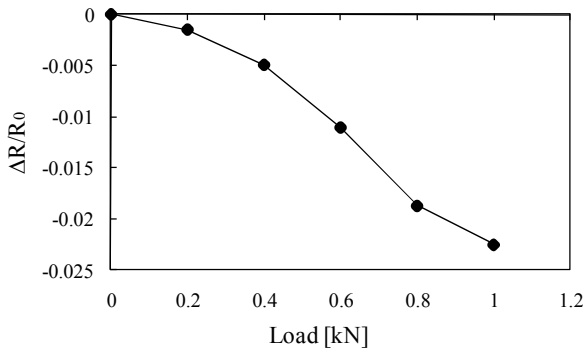

Fig. 12 Effect of indentation loading on electrical resistance change ratio

As shown in Fig. 11, the indentation does not cause bending stress in the specimen. Although a dent on the surface is not observed by visual inspection, the indentation load decreases the electrical resistance change ratio. Similar decreases have been reported in a previous paper [20]. Let us consider that the CFRP laminate is modeled as a parallel circuit of electrical resistances: each layer is considered to be an electrical resistance. The indentation causes a new electrical contact. That makes a new circuit serially connected parallel resistance circuit. This change may decrease the electrical resistance. Although the mechanism is not clear, this indentation load affects the decrease of the electrical resistance change ratio. The non-linear behavior over 500×10^{-6} for the four-point bending and 100×10^{-6} for the three-point bending is not a characteristic caused by the applied compression strain. This effect of the indentation must be carefully considered for any types of bending test specimens of CFRP.

Fig. 13 Compression side surface before loading

From 2000×10^{-6} for the three-point bending test, the electrical resistance change ratio increases gradually up to the point of fiber micro-buckling. To investigate the mechanism, surface observation was performed after loading to 2000×10^{-6}. Figure 13 shows the observation of the initial surface of the compression side of the CFRP near the indentation point with a video microscope. Figure 14 shows the observation result after loading to 2000×10^{-6}. As shown in Fig. 14, the red circles indicate the fiber breakages. The gradual increase of the electrical resistance change ratio is caused by the fiber breakages: weak carbon fibers break early in the loading process.

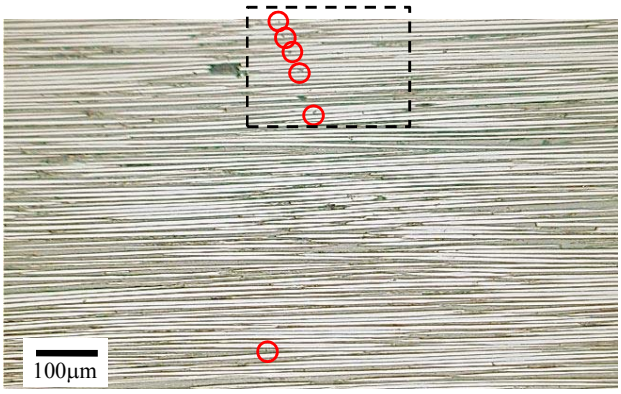

Fig. 14 Compression side surface after loading of 2000μ

4. Conclusions

This study dealt with the electrical resistance change of unidirectional CFRP under compression loading. Only a few research studies have been reported on compression

loading because of the difficulty of performing the experiments. This study started with the design of an appropriate test specimen that had a uniform electrical current, and by applying pure compression loading. A sandwich beam type specimen was adopted. The results obtained were as follows:

(1) Piezoresistivity under compression loading was identical to that of tension loading. The electrical resistance change ratio decreased linearly with the increase in applied compression load.
(2) Although fiber micro-buckling caused residual compression strain, the damage caused a significant increase in electrical resistance change ratio.
(3) Although the fiber micro-buckling caused complete fiber breakages, the increase of resistivity was only 120 times larger than that for the fiber direction of unidirectional CFRP.
(4) Fiber breakages caused a gradual increase in electrical resistance change ratio.
(5) Indentation loading caused a decrease in electrical resistance change ratio. This effect must be carefully considered for bending type specimens.

References

(1) K. Schulte, and Ch. Baron, Load and failure analyses of CFRP laminates by means of electrical resistivity measurement, Composites Science and Technology, 36(1), (1989) pp.63-76.
(2) N. Muto, H. Yanagida, T. Nakatsuji, M. Sugita, and Y. Ohtsuka, Preventing fatal fractures in carbon-fiber glass-fiber-reinforced plastic composites by monitoring change in electrical resistance, J. Am. Ceram. Soc.,76(4), (1993), pp.875-879.
(3) X. Wang and D.D.L. Chung, Sensing delamination in a carbon fiber polymer-matrix composite during fatigue by electrical resistance measurement, Polymer Composites, 18(6) ,(1997), pp.692-700.
(4) P.E. Irving and C. Thiagarajan, Fatigue damage characterization in carbon fibre composite materials using an electrical potential technique, Smart materials and structures, 7(4), (1998), pp.456-466.
(5) J.C. Abry, S. Bochard, A. Chateauminois, M. Salvia and G. Giraud, In situ detection of damage in CFRP laminates by electrical resistance measurements, Composites Science and Technology, 59(6), (1999), pp.929-935.
(6) D.C. Seo and J.J. Lee, Damage detection of CFRP laminates using electrical resistance measurement and neural network, Composite structures, 47(1-4), (1999), pp.525-530.
(7) S. Wang and D.D.L. Chung, Piezoresistivity in continuous carbon fiber polymer-matrix composite, Polymer Composites, 21(1), (2000), pp.13-19.
(8) R. Schueler, S.V. Joshi and K. Schulte, Damage detection in CFRP by electrical conductivity mapping , Composites Science and Technology, 61(6), (2001),pp.921-930.
(9) J. B. Park, T. Okabe, N. Takeda and W. A. Curtin, Electromechanical modeling of unidirectional CFRP composites under tensile loading condition, Composites Part A, 33(2), (2002), pp.267-275.
(10) K. Ogi and Y. Takao, Characterization of piezoresistance behavior in a CFRP unidirectional laminate, Composites Science and Technology, 65(2), (2005),pp.231-239.
(11) A. Todoroki, and J. Yoshida, Electrical resistance change of unidirectional CFRP due to applied load , JSME International J., Series A, 47,3,(2004)pp. 357-364.
(12) A. Todoroki, Y. Samejima, Y. Hirano, and R. Matsuzaki, Piezoresistivity of Unidirectional Carbon/epoxy Composites for Multiaxial Loading, Composites Science and Technology,69, 11, (2009), pp.1841-1846.
(13) A. Todoroki, K. Omagari, Y. Shimamura, and H. Kobayashi, Matrix crack detection of CFRP using electrical resistance change with integrated surface probes, Composites Science and Technology, Vol.66, No.11-12, (2006), pp 1539-1545.

(14) A. Todoroki, Y. Tanaka, and Y. Shimamura, Delamination monitoring of graphite/epoxy laminated composite plate of electrical resistance change method, Composites Science and Technology, 62(9),(2002), pp.1151-1160.
(15) A. Todoroki, M. Tanaka, and Y. Shimamura, Measurement of orthotropic electrical conductance of CFRP laminates and analysis of the effect on delamination monitoring with electrical resistance change method, Composites Science and Technology, 62(5), (2002), pp.619-628.
(16) A. Todoroki, M. Tanaka and Y. Shimamura, High performance estimations of delamination of graphite/epoxy laminates with electrical resistance change method, Composites Science and Technology, 63(13), (2003), pp.1911-1920.
(17) A. Todoroki, Y. Samejima, Y. Hirano, R. Matsuzaki and Y. Mizutani, Mechanism of electrical resistance change of a thin CFRP beam after delamination cracking, J. of Solid Mechanics and Materials Engineering, JSME, (to be published).
(18) Zhen Mei, Victor H. Guerrrero, Daniel P. Kowalik and D.D.L. Chung, Mechanical damage and strain in carbon fiber thermoplastic-matrix composite, sensed by electrical resistivity measurement, Polymer Composites, 23(3), (2002), pp.425-432.
(19) Shoukai Wang and D.D.L. Chung, Self-sensing of flexural strain and damage in carbon fiber polymer-matrix composite by electrical resistance measurement, Carbon, 44(13), (2006), pp.2739-2751
(20) Akira Todoroki, Kensuke Suzuki, Yoshihiro Mizutani and Ryosuke Matsuzaki, Durability estimations of Copper Plating Electrodes for Self-sensing CFRP Composites, Journal of Solid Mechanics and Materials Engineering, JSME, Vol.4, No.6, (2010)pp.